

# *EUVE* Observations of AR Lacertae: The Differential Emission Measure and Evidence for Extended Prominences

FREDERICK M. WALTER

Department of Earth and Space Sciences, SUNY, Stony Brook, NY 11794–2100, USA

*EUVE* observed the eclipsing RS CVn system AR Lac in October 1993. The differential emission measure shows a double-peaked structure similar to the two-temperature distribution seen in X-rays. The best-fit Fe abundance is 0.4 solar. The DS light curve shows a deep primary eclipse. The slow egress from eclipse may be due the presence of spatially extended, optically-thick “prominences” in the equatorial plane of the K star.

## 1. Introduction and Observations

All late-type stars, so far as we know, possess magnetic fields and the consequent phenomena termed “solar-like activity.” This activity results in non-radiative heating of the outer atmosphere, and the outwardly increasing temperatures that manifest themselves as chromospheres, transition regions, and coronae. We know far less about this non-radiative heating mechanism than we would like, even in the case of the Sun. Studies of how the emissions vary with stellar parameters (mass, rotation, age) give some clues to the coupling of the heating to the magnetic fields. Studies of the differential emission measure (DEM) tell us of how the energy is deposited in the stellar atmosphere.

I observed the well-studied active star, AR Lacertae, with the *EUVE* to determine the DEM for comparison with the X-ray and UV measurements. AR Lacertae (HD210334) is the brightest eclipsing RS CVn system known, with a 1.983 day orbital period.

The *EUVE* observed AR Lac on 12–15 October 1993. The first half of the observation was made with the target located at the nominal boresight (which by then was known to have suffered reduced sensitivity). For the latter half of the observation, the target was offset to two other positions [(-0.5', -10.8'), (+1.1', -5.4')] for boresight calibrations. Data were obtained over 48 spacecraft orbits. The total time in the observation is 104 ks.

The spectra were extracted at CEA, using IRAF/APEXTRACT, with the variance-weighting method. Lines Fe XVI through Fe XXIV are present (see Table 1).

The interstellar column  $n_{\text{H}}$  has generally been assumed to be  $10^{19} \text{ cm}^{-2}$  for X-ray spectral fits. I estimated  $n_{\text{H}}$  from the  $\lambda\lambda 335, 360 \text{ \AA}$  Fe XVI line ratio. The ratio of emissivities  $\frac{\lambda_{335}}{\lambda_{360}}$  is 2.14, independent of temperature or density. The observed ratio of  $2.72 \pm 0.84$  implies  $n_{\text{H}} = 1.8_{-1.8}^{+1.9} \times 10^{18} \text{ cm}^{-2}$ .

## 2. The Emission Measure Distribution

I used the *EUVE*\_FIT software, written by R.A. Stern, to fit the spectrum. The code simultaneously fits the emission line fluxes and the continuum intensity, yielding a DEM and the iron abundances. The ratio of the emission lines to the continuum is proportional to the metallicity  $[\frac{\text{Fe}}{\text{H}}]$ . The best fit DEM is shown in Figure 1.

The two-component thermal fits to the X-ray spectra, overplotted in Figure 1, agree remarkably well with the DEM from *EUVE*. The Ottmann et al. (1993) fit used a Raymond-Smith (1977) solar-abundance plasma; the *ASCA* and my PSPC fits use the MEKA code (Kaastra 1992) with the abundances as free parameters.

TABLE 1. Measured line fluxes

$\lambda_{\text{obs}}$	Line ID	$\lambda_{\text{pred}}^{\dagger}$	Flux $^{\ddagger}$	$\lambda_{\text{obs}}$	Line ID	$\lambda_{\text{pred}}$	Flux
90.80	Fe XIX	91.02	$3.2 \pm 0.2$	121.73	Fe XX	121.83	$4.1 \pm 0.4$
93.80	Fe XVIII	93.92	$9.4 \pm 0.4$	128.53	Fe XXI	128.73	$7.8 \pm 0.6$
97.73	Fe XXI	97.88	$0.9 \pm 0.2$	132.69	Fe XXIII	132.85	$30.1 \pm 2.0$
101.55	Fe XIX	101.55	$2.5 \pm 0.3$	135.65	Fe XXII	135.78	$5.7 \pm 0.6$
102.49	Fe XXI	102.22	$1.7 \pm 0.3$	142.08	Fe XXI	142.27	$3.4 \pm 0.9$
103.98	Fe XVIII	103.94	$1.7 \pm 0.2$	192.32	Fe XXIV	192.04	$18.5 \pm 1.5$
108.26	Fe XIX	108.37	$5.8 \pm 0.5$	256.41	He II	256.32	$3.5 \pm 0.5$
109.72	Fe XIX	109.97	$0.6 \pm 0.2$	284.89	Fe XV	284.15	$2.5 \pm 0.5$
117.03	Fe XXII	117.17	$14.7 \pm 1.0$	303.89	He II	303.91	$63.9 \pm 2.6$
118.60	Fe XX	118.66	$2.5 \pm 0.3$	335.30	Fe XVI	335.41	$7.9 \pm 1.5$
119.81	Fe XIX	120.00	$1.5 \pm 0.3$	359.93	Fe XVI	360.80	$2.9 \pm 0.7$

$^{\dagger}$  Line list from Brickhouse et al. 1995.

$^{\ddagger}$  Fluxes in units of  $10^{-14}$  erg  $\text{cm}^{-2}$   $\text{s}^{-1}$ .

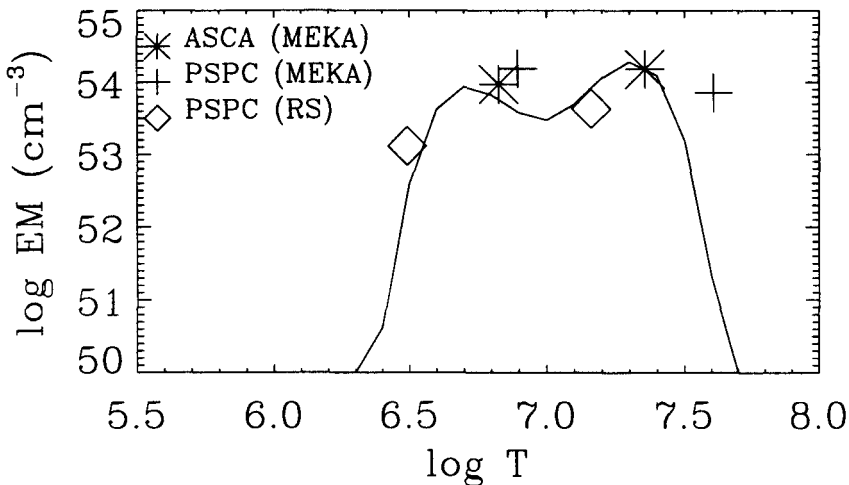


FIGURE 1. The differential emission measure (DEM) from the *EUVE* (continuous curve). The emission measures and temperatures from two component thermal fits to X-ray spectra are overlaid.

### 2.1. The Iron Abundance

The best estimate of  $\frac{Fe}{H}$  is 0.39 solar. Sub-solar abundances are routinely observed in *ASCA* X-ray spectra (e.g., White et al. 1994), and even *ROSAT* PSPC spectral fits for active stars are greatly improved if the abundances are permitted to fall below solar. These low abundances have been explained away as an artifact of incomplete line lists in the models (the Fe L transitions, which contribute significantly around 1 keV, are missing): the missing lines are modeled as continuum, leading to low line-to-continuum

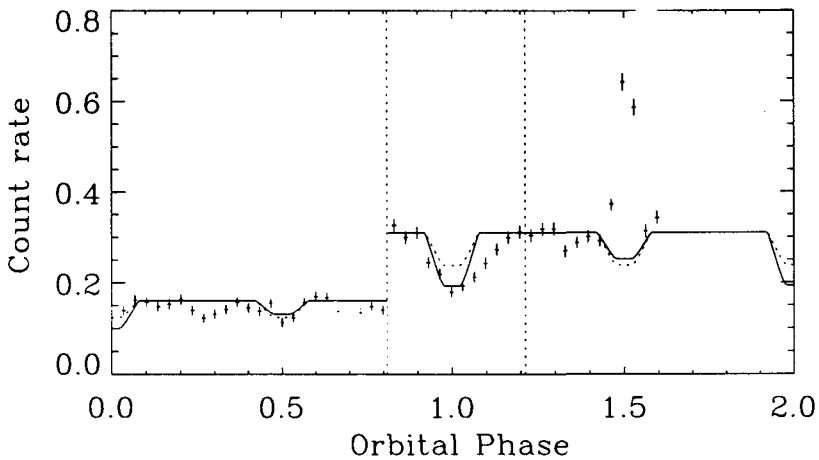


FIGURE 2. The DS light curve, plotted versus binary phase. The dotted vertical lines separate intervals with different boresight offsets. The low count rate in the first interval is due to the reduced sensitivity at the original boresight location. The solid line is the optical light curve, scaled to the mean out-of-eclipse level. Purely geometrical eclipses (the dotted line) are shallower. Primary eclipse has a depth of 42%, and is clearly asymmetric on egress. A flare coincides with secondary minimum.

ratios. *EUVE* spectra should not be subject to this problem, so the low abundance is somewhat of a mystery.

As the DEM fitting procedure weights all points by their errors, and the continuum points greatly outnumber the lines, it is possible that the criterion used to signal convergence of the fit is relatively insensitive to the lines. I checked this by artificially enhancing the S/N for the lines, to no avail. I then ran models at a range of  $n_{\text{H}}$ . Since the mean wavelength of the continuum is shorter than that of the lines, the line-to-continuum ratio depends on the assumed  $n_{\text{H}}$ . For  $n_{\text{H}} = 7 \times 10^{18} \text{ cm}^{-2}$  the best fit abundance does reach solar. However, examination of the fits shows that fits with  $n_{\text{H}} \geq 4 \times 10^{18} \text{ cm}^{-2}$  greatly underestimate the fluxes of the lines longward of  $\sim 250 \text{ \AA}$ .

Could this metal abundance deficiency be real? Naftilan & Drake (1977) claimed that the K star was metal-deficient relative to the Sun by about 1 dex, while the G star showed solar abundances. They note that is difficult to understand how the two stars in a close binary can have different abundances. Randich et al. (1993) show that many RS CVn systems appear underabundant in  $[\frac{\text{Fe}}{\text{H}}]$ , but suggest that the weak Fe lines are more likely a consequence of chromospheric emission which fills in the lines than of real underabundances. Both components of AR Lac are chromospherically active.

### 3. The Light Curve

The DS light curve is shown in Figure 2. The dotted vertical lines divide the regions with different boresight offsets. The loss in sensitivity the DS suffered in February 1993 is evident from the low count rate seen in the first half of the observation. The steep

spatial gradient of the sensitivity loss could account for most, if not all, of the apparent variations during that time. The light curve during the latter half of the observation clearly shows primary minimum; secondary minimum coincides exactly with a flare.

The residual intensity at primary minimum is  $58\% \pm 4\%$  of that outside eclipse. A purely geometrical eclipse of emitting regions with small scale heights would yield an eclipse depth of 33%. The mean surface flux of the emission from the G star must be  $2.5 \times$  that of the K star. Note that the EUV light curve is asymmetric with respect to primary minimum. The emission returned to the pre-eclipse level only slowly.

The depth of primary eclipse is similar to that seen with *Einstein* (Walter et al. 1983), *EXOSAT* (White et al. 1990), *ROSAT* (Ottmann et al. 1993), and *ASCA* (White et al. 1994). This is not surprising, as all instruments are probing similar coronal temperatures.

### 3.1. The Asymmetric Egress from Primary Minimum

There is deficiency of emission from the G star upon egress from primary eclipse. Such asymmetric light curves have been seen before in the *EXOSAT* LE light curve (White et al. 1990), the *ASCA* light curve (White et al. 1994), and the spectrally-resolved Mg II light curve (Neff et al. 1989).

The attenuation is highest close to the star, and falls slowly, reaching zero by phase 0.2 (projected separation  $5.8 R_K$ ). If the attenuation is caused by absorption or scattering, the responsible material must extend a significant fraction of the distance between the stars. Four possible explanations for the slow egress from primary minimum are:

**Enhanced photoelectric absorption on the line of sight:** The maximum  $n_H$  necessary to produce the observed attenuation is just over  $10^{19} \text{ cm}^{-2}$ . The neutral hydrogen can exist either (a) within an extended and presumably hot corona, or (b) in a cool extended region well above the K star. Possibility a conflicts with the inferred coronal emission measure  $n_e^2 V$ . For a neutral fraction of  $10^{-6}$ , the total column is of order  $10^{24-25} \text{ cm}^{-2}$ . Over a length of order  $2R_K$ , this requires coronal densities  $n_e \sim 10^{12} \text{ cm}^{-3}$  and  $n_e^2 V \sim 10^{60} \text{ cm}^{-3}$ , which exceeds all coronal emission measure estimates by some 7 orders of magnitude. For possibility b, I assume  $n_e = 10^{10} \text{ cm}^{-3}$  (Solar prominences have densities up to  $10^{12}$ ). This requires a path length of order  $10^8$  to  $10^9 \text{ cm}$ , which is appropriate for a prominence. However, the scale height of the prominence exceeds  $10^{11} \text{ cm}$ , since it must cover the entire surface area of the G star. The absorbing structure must then be a thin sheet parallel to our line of sight, which seems unlikely.

**Enhanced electron scattering on the line of sight:** This possibility is attractive inasmuch as the X-ray, EUV, and Mg II light curves appear similar, despite the different sensitivities to interstellar absorption.  $\tau = 1$  for electron scattering requires  $n_H \sim 10^{24} \text{ cm}^{-2}$ . Over a path length of order  $2R_K$ ,  $n_e$  must exceed  $10^{12} \text{ cm}^{-3}$ , which leads to the same absurdly large volume emission measures discussed above.

**Reduced emission on the visible hemisphere of the G star:** The attenuated flux is observed over an interval of only 0.2 in phase. There is no evidence that the emission from the G star varies at any other phase. It is not possible to construct a surface intensity distribution that is constant for 80% of a cycle and dips for the other 20%. While it is possible to contrive such a light curve using patchy flux distributions on both stars (e.g., White et al. 1990), I consider this an unlikely and ad-hoc explanation.

**Geometric obscuration by optically thick material:** If the obscuring material is optically thick (say,  $n_H > 10^{22}$ ), but only obscures a portion of the G star, then one would see similar attenuations in *EUVE* and *ASCA*. Cool, dense material confined within  $15^\circ$  of equator of the K star, and extending outward by  $\sim R_K$ , could account for the observed attenuation by geometrical obscuration alone (Figure 3). The inferred  $n_e$

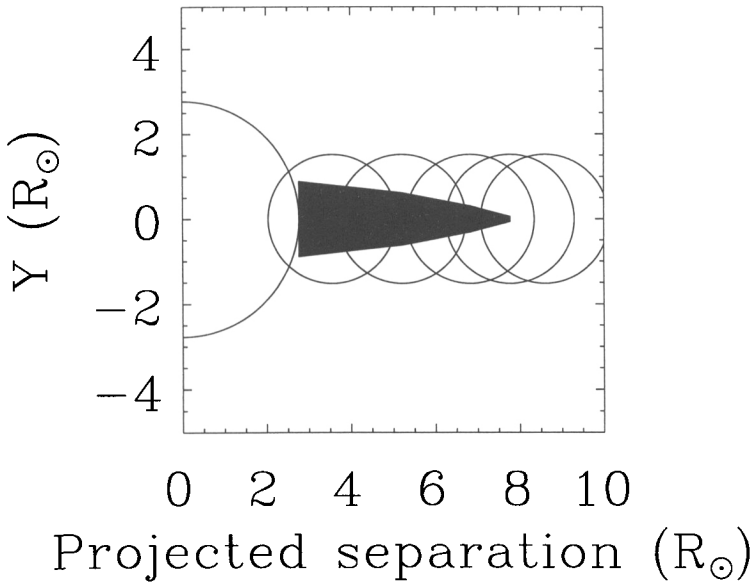


FIGURE 3. Simple geometrical model of the obscuration needed to account for the attenuation seen on egress from primary eclipse. The G star is plotted at the five phases observed following primary minimum. The shaded area is optically thick.

is from  $10^{11}$  to  $10^{12}$   $\text{cm}^{-3}$ , which is similar to that seen in some solar prominences. Such cool structures would not contribute to the coronal emission measure. There is growing evidence for such large structures in active stars (Linsky 1994).

I am indebted to Bob Stern for donating his *EUVE* line + continuum fitting code, and to Jürgen Schmitt for useful discussions about MADs. I thank the staff at CEA for assisting me with the preliminary data reductions. Lastly, we must acknowledge Stu Bowyer for his persistence, which ensured the success of the *EUVE*.

#### REFERENCES

- BRICKHOUSE, N. S., RAYMOND, J. C., & SMITH, B. W. 1995, *ApJS*, in press
- KAastra, J. S. 1992, *An X-Ray Spectral Code for Optically Thin Plasmas* SRON-Leiden Report
- LINSKY, J. L. 1994, in *Solar Coronal Structures*, ed. V. Ruslin, P. Heinzel, & J.-C. Vial, 641
- NAFTILAN, S. A. & DRAKE, S. A. 1977, *ApJ*, 216, 508
- NEFF, J. E., ET AL. 1989, *A&A*, 215, 79
- OTTMANN, R., SCHMITT, J. H. M. M., & KÜRSTER, M. 1993, *ApJ*, 413, 710
- RANDICH, S., GRATTON, R., & PALLAVICINI, R. 1993, *A&A*, 273, 194
- RAYMOND, J. C. & SMITH, B. W. 1977, *ApJS*, 35, 419
- WALTER, F. M., GIBSON, D. M., & BASRI, G. S. 1983, *ApJ*, 267, 665
- WHITE, N. E., SHAFER, R. A., HORNE, K., PARMAR, A. N., & CULHANE, J. L. 1990, *ApJ*, 350, 776
- WHITE, N. E., ARNAUD, K., DAY, C. S. R., EBISAWA, K., GOTTHELF, E. V., MUKAI, K., SOONG, Y., YAQOUB, T., & ANTUNES, A. 1994, *PASJ*, 46, L97